

***O*- and *N*-Glycosylation of Serum Immunoglobulin A is Associated with IgA Nephropathy and Glomerular Function**

Viktoria Dotz^{1,#,*}, Alessia Visconti^{2,*}, Hannah J Lomax-Browne^{3,*}, Florent Clerc^{1,*}, Agnes L Hipgrave Ederveen¹, Nicholas R Medjeral-Thomas³, H. Terence Cook³, Matthew C Pickering³, Manfred Wuhrer^{1,+}, Mario Falchi^{2,+,\$}

¹Center for Proteomics and Metabolomics, Leiden University Medical Center (LUMC), Leiden, The Netherlands

²Department of Twin Research & Genetic Epidemiology, King's College London, London, United Kingdom

³Centre for Inflammatory Disease, Department of Medicine, Imperial College London, London, United Kingdom;

#Current address: Janssen Vaccines & Prevention, Leiden, The Netherlands

*These authors contributed equally to this work

+These authors share senior authorship.

\$Corresponding author: Mario Falchi, mario.falchi@kcl.ac.uk

Keywords: IgA Nephropathy, glycosylation, immunoglobulin, mass spectrometry, posttranslational modification

Abstract

Background Immunoglobulin A (IgA) nephropathy (IgAN) is the most common primary glomerular disease worldwide, and is a leading cause of renal failure. The disease mechanisms are not completely understood, but a higher abundance of galactose-deficient IgA is recognized to play a crucial role in IgAN pathogenesis. While both types of human IgA (IgA1 and IgA2) have several *N*-glycans as posttranslational modification, only IgA1 features extensive hinge-region *O*-glycosylation. IgA1 galactose-deficiency on the *O*-glycans is commonly detected by a lectin-based method. To date, limited detail is known about IgA *O*- and *N*-glycosylation in IgAN.

Methods To gain insights into the complex *O*- and *N*-glycosylation of serum IgA1 and IgA2 in IgAN, we employed liquid chromatography-mass spectrometry (LC-MS) for the analysis of tryptic glycopeptides of serum IgA from 83 IgAN patients and 244 age and sex-matched healthy controls.

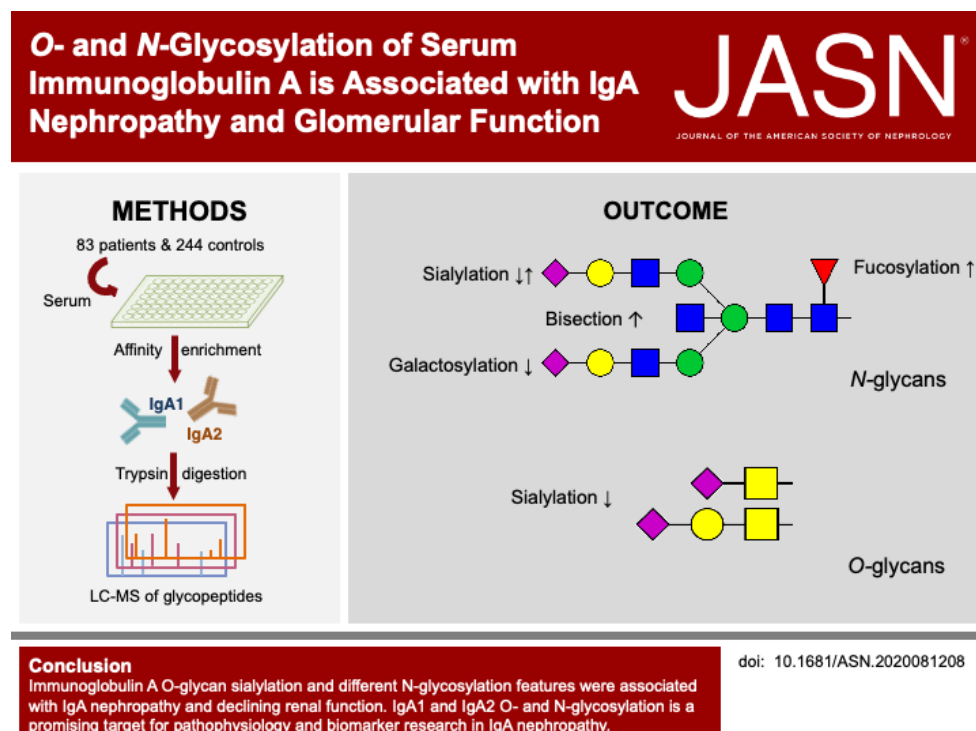
Results Multiple structural features of *N*-glycosylation of IgA1 and IgA2 were associated with IgAN and glomerular function in our cross-sectional study. This included differences in galactosylation, sialylation, bisection, fucosylation, and *N*-glycan complexity. Moreover, IgA1 *O*-glycan sialylation was associated with both disease risk and glomerular function. Finally, glycopeptides were a better predictor of IgAN and glomerular function than galactose-deficient IgA1 levels measured by lectin-based ELISA.

Conclusions Our high-resolution data suggest that IgA *O*- and *N*-glycopeptides are promising targets for future investigations on the pathophysiology of IgAN and as potential noninvasive biomarkers for disease prediction and deteriorating kidney function.

Significance Statement

IgA nephropathy (IgAN) is the commonest primary glomerular disease worldwide with galactose deficient IgA (gd-IgA) being considered to play a key role in its pathogenesis. While this is widely reported, it is unclear how IgA glycosylation changes with disease. The use of a novel mass spectrometry-based approach allowed obtaining a more complete picture of IgA glycosylation changes in IgAN, and of the relationship between IgA glycosylation and kidney function. Multiple structural features of both *O*- and *N*-linked glycans were associated with the presence and severity of IgAN and kidney function. Our high-resolution data suggest that IgA *O*- and *N*-glycopeptides are promising targets for future studies on the pathophysiology of IgAN and as potential noninvasive biomarkers for disease prediction.

Graphical abstract



Introduction

Immunoglobulin A (IgA) nephropathy (IgAN), or Berger's disease, is the most common glomerulonephritis worldwide (1). The disease course is complex, varying from a mild form to a progressive disease leading to renal failure in up to 40% of patients within 20 years (1,2). Clinical presentation also differs greatly with gender, ethnicity, and age (1). IgAN is diagnosed by the presence of IgA dominant or co-dominant mesangial deposits on renal biopsy (3). Improved, noninvasive biomarkers of disease severity and progression to chronic kidney disease are needed to appropriately stratify patient treatment and develop novel, effective therapies.

IgAN pathogenesis is generally considered to follow the “four-hit hypothesis” (4). In this hypothesis, the pathogenesis is initiated by increased levels of circulating galactose-deficient IgA1 (gd-IgA; hit 1). gd-IgA is then recognized by anti-glycan autoantibodies (hit 2), leading to the formation of immune complexes (hit 3) that may deposit in the kidney (hit 4) and cause glomerular inflammation, complement activation, and kidney injury (4).

IgA1, unlike IgA2, has a unique hinge region located between conserved regions 1 and 2 of the heavy chain (5). The hinge region has 9 potential sites for O-glycosylation, of which 3-6 are reported to be consistently glycosylated (6-8). O-glycans located in the hinge region of IgA1 are typically core 1 glycans with the structure galactose β 1-3N-acetylgalactosamine (GalNAc), which may be extended with up to two sialic acid residues (6) (**Figure 1**). In IgAN patients regardless of ethnicity or age, an increased proportion of the IgA1 hinge region O-glycans lack galactose (gd-IgA) and terminate, instead, in GalNAc or sialylated GalNAc (9-13). The gd-IgA levels are elevated in patients with progressive IgAN compared to stable patients, and a negative correlation between gd-IgA level and the estimated glomerular filtration rate (eGFR) has been found (12).

Measurement of gd-IgA in blood samples is typically achieved by ELISA incorporating the use of a lectin, *Helix aspersa* agglutinin (HAA), which recognizes terminal GalNAc residues on *O*-glycans. Another lectin, Jacalin, is often used to isolate IgA from samples for further analysis. Whilst lectin-based approaches are useful tools in this aspect, variability in their specificities and interferences, especially by the co-presence of sialic acids, limit their robustness (14–16).

While aberrant *O*-glycosylation of gd-IgA in IgAN has been widely reported, not much is known about the role of *N*-glycans. Both IgA1 and IgA2 are *N*-glycosylated. IgA1 contains two *N*-linked glycosylation sites on each heavy chain (Asn263/Asn459) and IgA2 contains an additional two or three *N*-glycans (**Figure 1**). The *N*-glycans on IgA are reported to be mainly complex-type, digalactosylated diantennary structures (6,8). Elevated levels of sialylation (17) and mannosylation (18) of serum IgA1 *N*-glycans from IgAN patients have been identified. Moreover, mice with a gene knock-out (*β4GalT*) leading to agalactosylated *N*-glycans developed IgAN-like glomerular lesions upon IgA deposition (19).

Despite the involvement of IgA glycosylation in the pathogenesis of IgAN, it is still largely unclear how IgA glycosylation changes with disease. The molecular nature of IgA *O*- and *N*- glycosylation in IgAN has hitherto been incompletely explored. Here, we used our new mass spectrometry (MS) based approach for IgA *O*- and *N*-glycosylation analysis in a sizable case-control cohort to obtain a more complete picture on the IgA glycosylation changes in IgAN at an unprecedented level of detail and resolution and to further investigate the relationship of IgA glycosylation and kidney function.

Methods

Study Populations

IgA nephropathy patient samples were collected as part of the Causes and Predictors of Outcome in IgA Nephropathy Study, a retrospective cohort study ethically approved by the UK National Research Ethics Service Committee. All individuals provided informed written consent (14/LO/0155). Here, we investigated 83 unrelated patients from the UK with serum samples available and complete clinical follow-up at the time of recruitment (**Supplemental Table S1**). Estimated glomerular filtration rate (eGFR), estimated by CKD-EPI and corrected for body surface area, was used as a biomarker of renal function (12).

The control samples were randomly ascertained among healthy UK twins from the TwinsUK adult twin registry (20), and age- and sex-matched with the IgA nephropathy cases (**Supplemental Figure S1**). The sample included 244 individuals (49 monozygotic and 64 dizygotic twin pairs, and 18 singletons; **Supplemental Table S1**). St. Thomas' Hospital Research Ethics Committee approved this study, and all twins provided informed written consent.

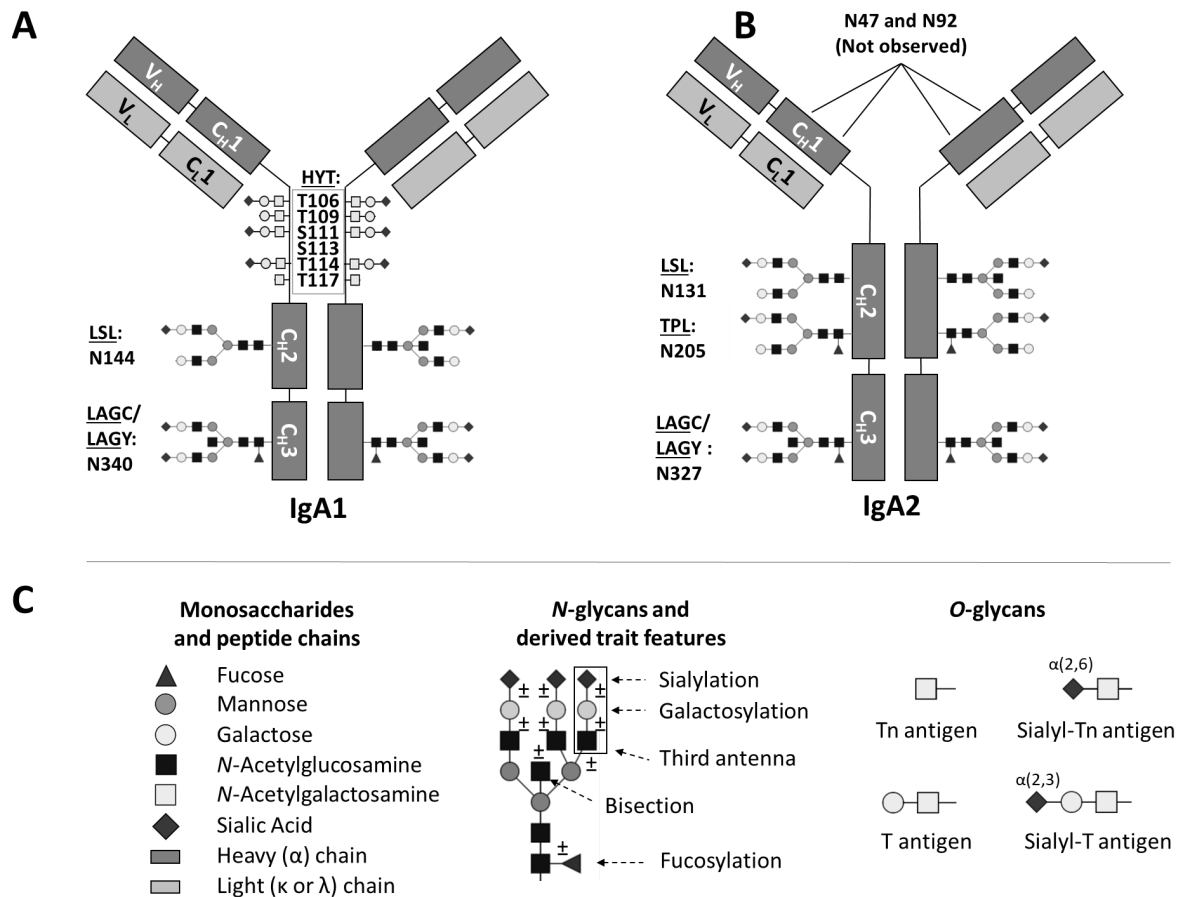


Figure 1. Schematic representation of IgA1 and IgA2 with examples for *O*- and *N*-glycan structures. **A.** Each IgA1 heavy chain contains two *N*-glycosylation sites, *i.e.*, at N144 and N340, which are occupied by complex-type *N*-glycans, next to six *O*-glycosylation sites, *i.e.*, at T106, T109, S111, S113, T114, and T117. All six *O*-glycosylation sites in the hinge-region of IgA1 are present on a single tryptic peptide (HYT) (6,8). **B.** With our MS-based approach, we observed three different *N*-glycosylation sites on IgA2, *i.e.*, at N131, N205 and N327, which were occupied with complex-type *N*-glycans. Glycopeptides indicating glycosylation on the two other potential *N*-glycosylation sites were not detected in our study. **C.** Symbols and example structures of *O*- and *N*-glycans. In this work, we refer to the first three letters of the tryptic peptide sequence of the detected glycopeptides: HYT for the multiply *O*-glycosylated hinge-region peptide, LSL for the glycopeptide with the *N*-glycosylation site N144 or N131 on IgA1 or IgA2, respectively, TPL for the glycopeptide with the IgA2 *N*-glycosylation site N205, LAG for the glycopeptide with the *N*-glycosylation site N340/N327 on IgA1/IgA2, which was detected with either a terminal tyrosine (LAGY), or as truncated form (LAGC). Glycosylation site numbering according to UniProtKB. Figure modified from (55).

Measurement of Serum IgA and gd-IgA Levels

Serum IgA levels were measured using enzyme-linked immunosorbent assay (ELISA) as previously described (21). The capture antibody was the F(ab')₂ fragment goat anti-human IgA (Jackson Immuno-Research, West Grove, PA), and the detection antibody was the F(ab')₂ fragment biotinylated goat anti-human IgA1 (Jackson Immuno-Research).

Serum gd-IgA1 levels were measured using a lectin-based ELISA as previously described (21). The capture antibody was a polyclonal rabbit antihuman IgA (Dako, Glostrup, Denmark). The detection involved *Helix aspersa* agglutinin-biotin (Sigma, Darmstadt, Germany), followed by poly-streptavidin horseradish peroxidase (Pierce, Waltham, MA).

The intraclass correlation coefficient for the IgA assay was 0.74 (95% confidence interval, 0.63–0.83), and that for the gd-IgA1 assay was 0.89 (95% confidence interval, 0.73–0.95).

IgA glycopeptide analysis by mass spectrometry

A detailed description of the material and methods can be found in the **Supplemental Methods**. Briefly, serum samples from cases and controls, together with 22 pooled-plasma standards were pipetted onto 96-well plates in randomized manner. IgA were captured from 10 μ L of serum using CaptureSelectTM IgA affinity beads (ThermoFisher). (Glyco-)Peptides were generated by reduction, alkylation and digestion of the protein with trypsin. Tryptic digests were separated by reversed-phase nano-liquid chromatography (LC) on a C18 column (75 μ m \times 100 mm, particle size 1.7 μ m) and analyzed by mass spectrometry (MS) using an Impact HD quadrupole time-of-flight-MS system (Bruker Daltonics, Bremen, Germany) equipped with a nanoBooster, as previously described (22).

Raw LC-MS data were converted to mzXML using MSConvert. LaCyTools (23) (version 1.0.1) was used to align the LC runs, to calibrate (**Supplemental Table S2**) the mass spectra, and to extract glycopeptide signal intensities. For the extraction step, a previously reported list of potential IgA glycopeptide analytes was used (24–26), in addition to manual identification of glycoforms in the averaged spectra of 20 samples of both healthy individuals and patients.

Quality control was based on signal-to-noise, exact mass deviation, and isotopic pattern as described previously (23). 69 glycopeptides were retained and quantified. Their absolute signal intensities were normalized to the intensity sum of all glycopeptide species sharing the same tryptic peptide sequence, resulting in relative intensities. In this manuscript, IgA1 and IgA2 glycopeptide names are comprised by the letter codes of the first three amino acids of the peptide sequence: HYT, LSL, TPL and LAG, the last detected in two variants, i.e., as LAGC and LAGY (**Figure 1**). The peptide name is followed by the glycan composition indicating the number of hexoses (H), *N*-acetylhexosamines (N), fucoses (F), and sialic acids (S; **Supplemental Table S2**).

Structurally similar glycopeptides were summarized into 52 derived traits calculated from the relative intensities, as illustrated in **Supplemental Table S3**. For example, the abundances of all bisected diantennary structures within the TPL glycopeptide cluster were summed and divided by the sum of the abundances of all structures within the TPL cluster, resulting in the derived trait TPL_A2FB, bisection of fucosylated diantennary glycans with the formula: $A2FB = (H4N5F1S0 + H5N5F1S0 + H4N5F1S1 + H5N5F1S1 + H5N5F1S2) / (H4N5F1S0 + H5N5F1S0 + H5N4F1S1 + H4N5F1S1 + H5N5F1S1 + H5N4F1S2 + H5N5F1S2)$. Since each measured glycopeptide structure carries different types of monosaccharides, derived traits can give a more composite and robust measure of the different glycosylation features, i.e., for *N*-glycans (27), complexity/branching (diantennary vs triantennary), bisection, fucosylation, and, for both *O*- and *N*-glycans, galactosylation and sialylation.

Statistical analyses

The relative intensities of the detected glycopeptides and the derived trait values were corrected for batch effects (plate, plate row, and column) in R (version 3.3.3) using the function *ComBat* from the R package *sva* (release 3.2) on log-transformed data. Outliers, defined as measurements deviating more than three standard deviations from the mean of each trait, were removed. To ensure the normality of their distribution, the relative intensities of the detected glycopeptides as well as of the derived traits were quantile normalized.

gd-IgA level and IgAN status (case vs control) were tested for association with glycopeptides and derived traits using a linear mixed model using the function *lmer* from the R package *lmerTest* (version 3.1), including age, sex, and their interaction term as fixed effects, and family structure as a random effect, to correct for the non-independence of the twin observations. To avoid potential spurious associations due to differences in glycan composition between cases and controls, association with gd-IgA levels was assessed using healthy individuals only. eGFR (assessed in IgAN patients only) was

tested for association using a linear regression model (function *lm*, from the *stats* R package, version 3.6.1). Age, sex, and their interaction term were included as covariates.

Power calculation was performed using the *pwr* R package (version 1.3) and asking for the power to detect, in a sample of 83 cases and 244 controls, a Cohen's conventional medium effect size (28) of 0.5 of a standard deviation at an α -level of $0.05/(23 \times 3) = 7.3 \times 10^{-4}$ and $0.05/(16 \times 3) = 1.0 \times 10^{-3}$, for measured and derived traits, respectively.

We considered an association significant when its p-value passed a Bonferroni-derived threshold of $0.05/N_{\text{eff}}$, where N_{eff} is the effective number of independent tests taking into account the strong correlation among glycan relative intensities. N_{eff} was calculated using the approach proposed by Li & Ji (29) and multiplied by the number of phenotypes analyzed in this study. N_{eff} was $23(\times 3)$ for measured glycopeptides and $16(\times 3)$ for derived traits.

We further evaluated, for both IgAN and glomerular function, the predictive power of a model including only the gd-IgA serum levels, and a model including either the glycopeptides or derived traits significantly associated with IgAN/glomerular function. In this second model, due to the high correlation among traits, if two traits had a Pearson's correlation larger than 0.9, only the most significantly associated was used. Predictive powers were evaluated using the McFadden's adjusted pseudo- R^2 (30) (evaluated *via* the function *PseudoR2*, from the *DescTools* R package, version 0.99.39), for the binary trait IgAN, and adjusted R^2 , for the continuous trait eGFR (evaluated *via* the *lm* function). The adjusted values allow penalizing for the number of predictors in the model ($k=1$ when only gd-IgA levels are used, and $k>1$ when the glycopeptides or derived traits are used).

Results

Glycosylation features are associated with the level of gd-IgA in healthy individuals

As a first comparison of the traditional lectin-based method and our MS-based approach for measuring IgA glycosylation, we assessed the cross-sectional associations between gd-IgA values and MS-detected glycosylation traits. Using data from 236 healthy individuals, we found associations between gd-IgA and 26 out of 30 detected *O*-glycopeptides (HYT cluster) and all 7 derived *O*-glycan traits (**Supplemental Table S4**). The strongest associations were observed with decreased sialylation (HYT_nS, HYT_nS>nG, HYT_SperG) and galactosylation (HYT_GalperGalNAc and HYT_nGal), along with a relative increase of GalNAcylation (HYT_nGalNAc>nG and HYT_nGalNAc; **Figure 2**), which showed a similar trend in IgAN patients (**Supplemental Figure S2**). *N*-glycosylation traits from the LAGC cluster were also associated with gd-IgA, although to a lesser extent than *O*-glycosylation (**Supplemental Table S4**). Moreover, we compared the associations between gd-IgA and glycopeptides with and without correction for IgA1 titer, in a subset of 156 healthy individuals for whom IgA1 titer was available. IgA1 titer correction had negligible effects on the associations (**Supplemental Table S5**).

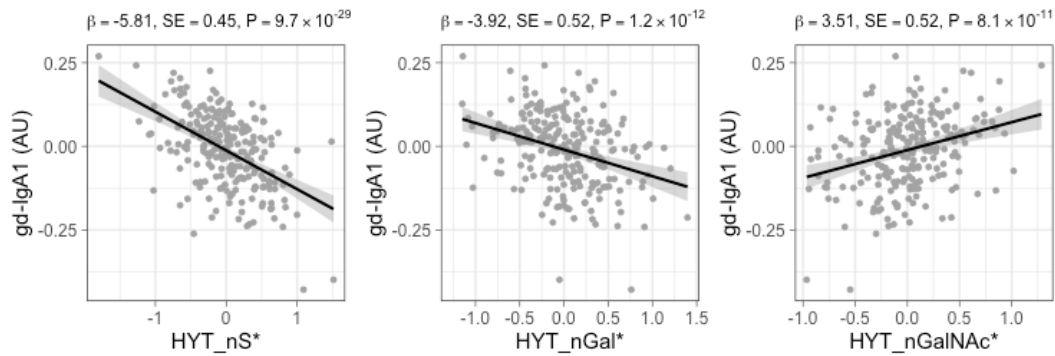


Figure 2. Main associations between derived *O*-glycosylation traits, and gd-IgA1 levels detected by HAA lectin in 236 healthy individuals. Quantile-normalised age- and sex-corrected values are plotted, and each scatterplot reports effect size (β), standard error (SE), and p-value (P) of the linear regression analysis. Derived traits HYT_nS, HYT_nGal, and HYT_nGalNAc correspond to average number of sialic acids, galactoses, and *N*-acetylgalactosamines, respectively. Monosaccharide symbols are depicted, in black and white, according with the nomenclature of the Consortium for Functional Glycomics, and were generated using GlycoWorkbench (56).

***O*- and *N*-glycosylation of IgA is associated with IgA nephropathy**

We used a case-control study design, including 83 IgAN patients and 244 healthy controls, to investigate cross-sectional associations between IgAN and IgA *O*- and *N*-glycosylation features detected by MS. Using 83 IgAN patients and 244 healthy controls we have $\geq 70\%$ power to detect a difference of 0.5 of a standard deviation between groups at a Bonferroni-derived p-value of $0.05/(23 \times 3) = 7.3 \times 10^{-4}$ and $0.05/(16 \times 3) = 1.0 \times 10^{-3}$, for measured and derived traits, respectively.

We found that galactosylation of the *N*-glycopeptides in the TPL and LSL clusters, next to sialylation in TPL and sialylation of the HYT *O*-glycopeptides, were lower in IgAN patients compared to controls, whereas bisection and sialylation in LSL, diantennary glycans in LAGCa, TPL, and LAGCb, and fucosylation in LAGCb were higher in patients (**Figure 3, Supplemental Table S6**).

***O*- and *N*-glycosylation of IgA is associated with renal function**

Using data from IgAN patients, we sought association between glycan traits and estimated glomerular filtration rate (eGFR), a marker of renal function. *N*-glycosylation features from all detected IgA glycopeptide clusters were associated with eGFR: bisection of LAGY, LSL, LAGC, and TPL was lower, while galactosylation and sialylation of TPL and LSL was higher in patients with higher eGFR (**Figure 4; Supplemental Table S7**). Regarding *O*-glycosylation, only sialylation showed significant, positive associations with eGFR (HYT_nS, HYT_SperG, and HYT_nS>nG), reflected in low levels of mono- or disialylated glycopeptides, e.g., HYT_H4N4F0S1, and high levels of multisialylated ones, e.g., HYT_H4N4F0S4 (**Figure 4, Supplemental Table S7**).

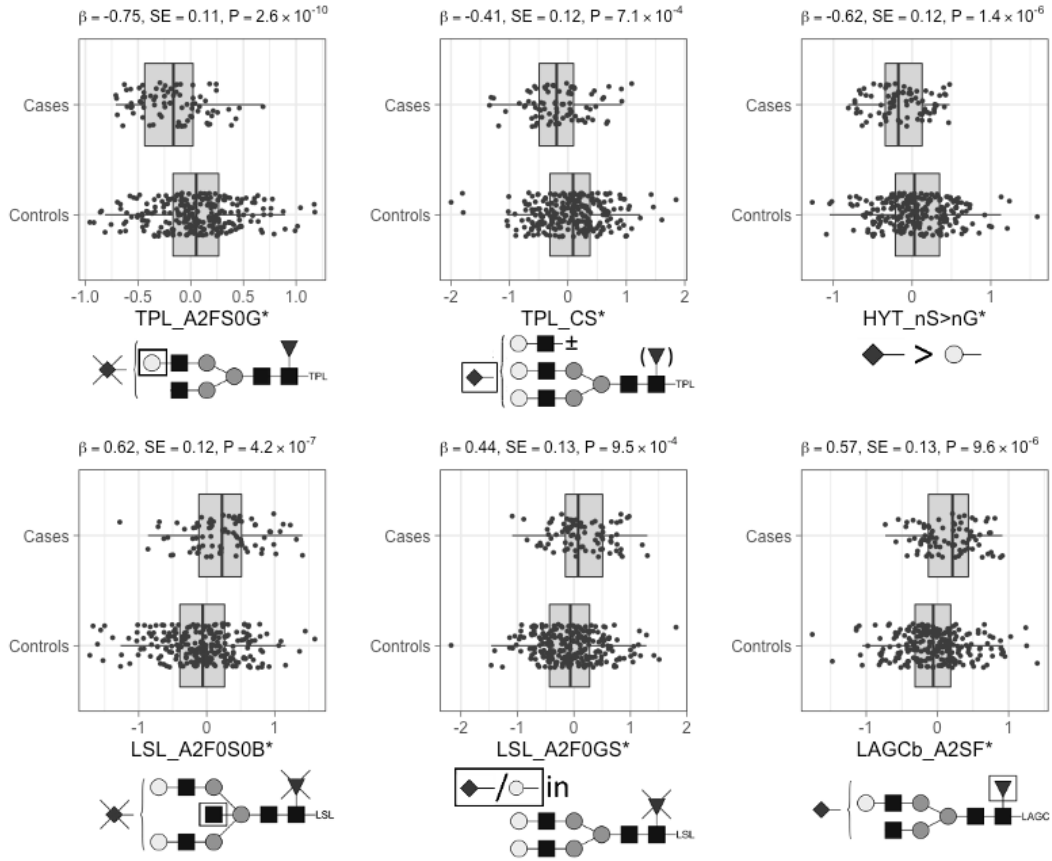


Figure 3. Main associations between derived glycosylation traits in serum IgA from healthy controls and individuals with IgA nephropathy (N=327). Quantile-normalised age- and sex-corrected values are plotted, and each boxplot reports effect size (β), standard error (SE), and p-value (P) of the regression analysis. Glycopeptide derived trait nomenclature refers to the first three letters of the tryptic amino acid sequence followed by the glycosylation features as calculated from detected glycopeptides (**Supplemental Table S3**); glycosylation traits: A2FS0G, galactosylation of non-sialylated fucosylated diantennary glycans; CS, sialylation within complex glycans; nS>nG, relative intensity sum of structures in which the number of sialic acids exceeds the number of galactoses; A2F0S0B, bisection of non-fucosylated non-sialylated diantennary; A2F0GS, sialic acid per galactose in non-fucosylated diantennary; A2SF, fucosylation of sialylated diantennary. Monosaccharide symbols are depicted, in black and white, according with the nomenclature of the Consortium for Functional Glycomics, and were generated using GlycoWorkbench (56).

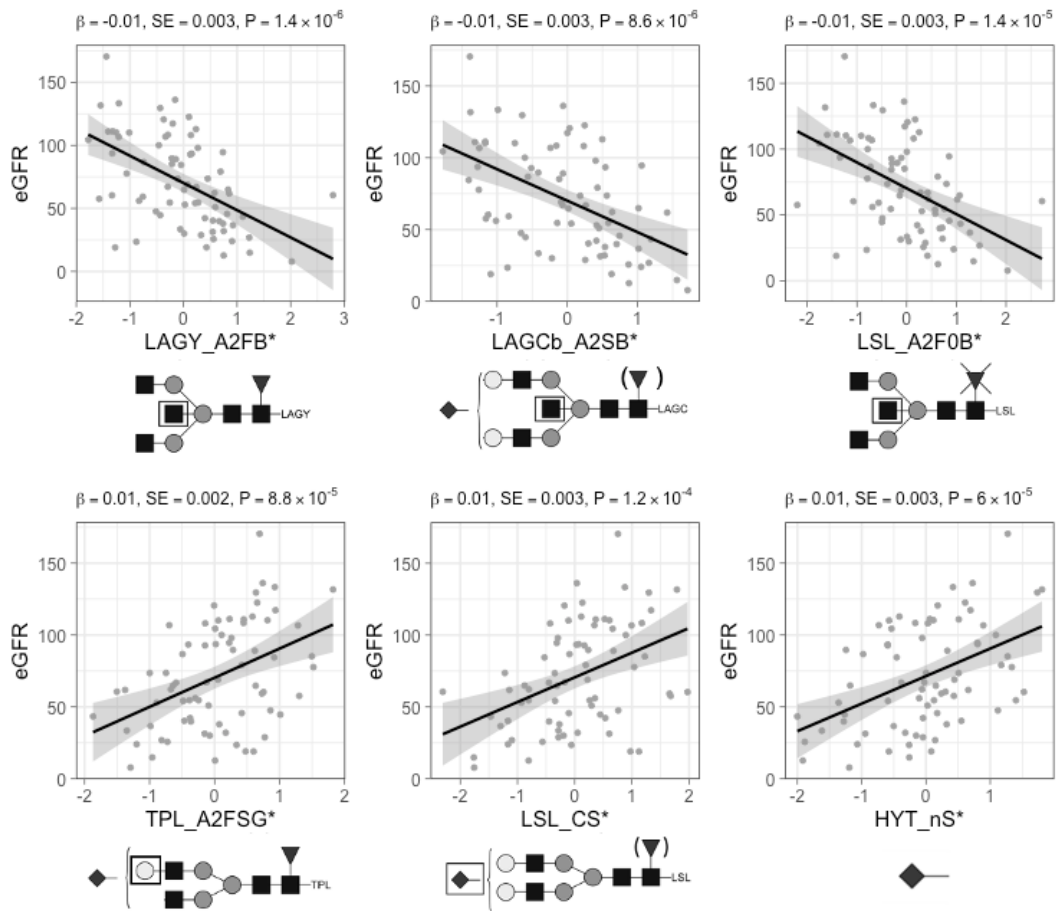


Figure 4. Main associations between IgA O-glycosylation traits and eGFR in 75 IgAN patients. Quantile-normalised age- and sex-corrected values are plotted, and each scatterplot reports effect size (β), standard error (SE), and p-value (P) for the linear regression analysis. Glycopeptide derived trait nomenclature refers to the first three letters of the tryptic amino acid sequence followed by the glycosylation features as calculated from detected glycopeptides (**Supplemental Table S3**); glycosylation traits: A2FB, bisection of fucosylated diantennary glycans; A2SB, bisection of sialylated diantennary; A2F0B, bisection of non-fucosylated diantennary; A2FSG, galactosylation of sialylated fucosylated diantennary; CS, sialylation within complex glycans; nS, average number of sialic acids. Glycan structures are reported below each panel. Monosaccharide symbols are depicted, in black and white, according to the nomenclature of the Consortium for Functional Glycomics, and were generated using GlycoWorkbench (56).

Glycopeptides and derived traits are better predictors of IgAN status and renal function than gd-IgA levels

Using McFadden's adjusted pseudo- R^2 (30) we found that glycopeptides and derived traits which were associated with IgAN from our analyses were better predictor of the disease than gd-IgA levels, with a pseudo- R^2 of 0.14, 0.12 and 0.02, for glycopeptides, derived traits, and gd-IgA levels, respectively. Analogously, glycopeptides and derived traits associated with eGFR showed a pseudo- R^2 of 0.23 and 0.22, respectively, vs 0.07 of gd-IgA levels. These results suggest that MS glycosylation data may not only give insights into the pathophysiology of IgAN but can also provide leads for noninvasive biomarkers for disease and deteriorating kidney function.

A summary of the major associations with gd-IgA, IgAN, and glomerular function is visualized in **Figure 5**, for derived traits, and **Supplemental Figure 3**, for measured glycopeptides.

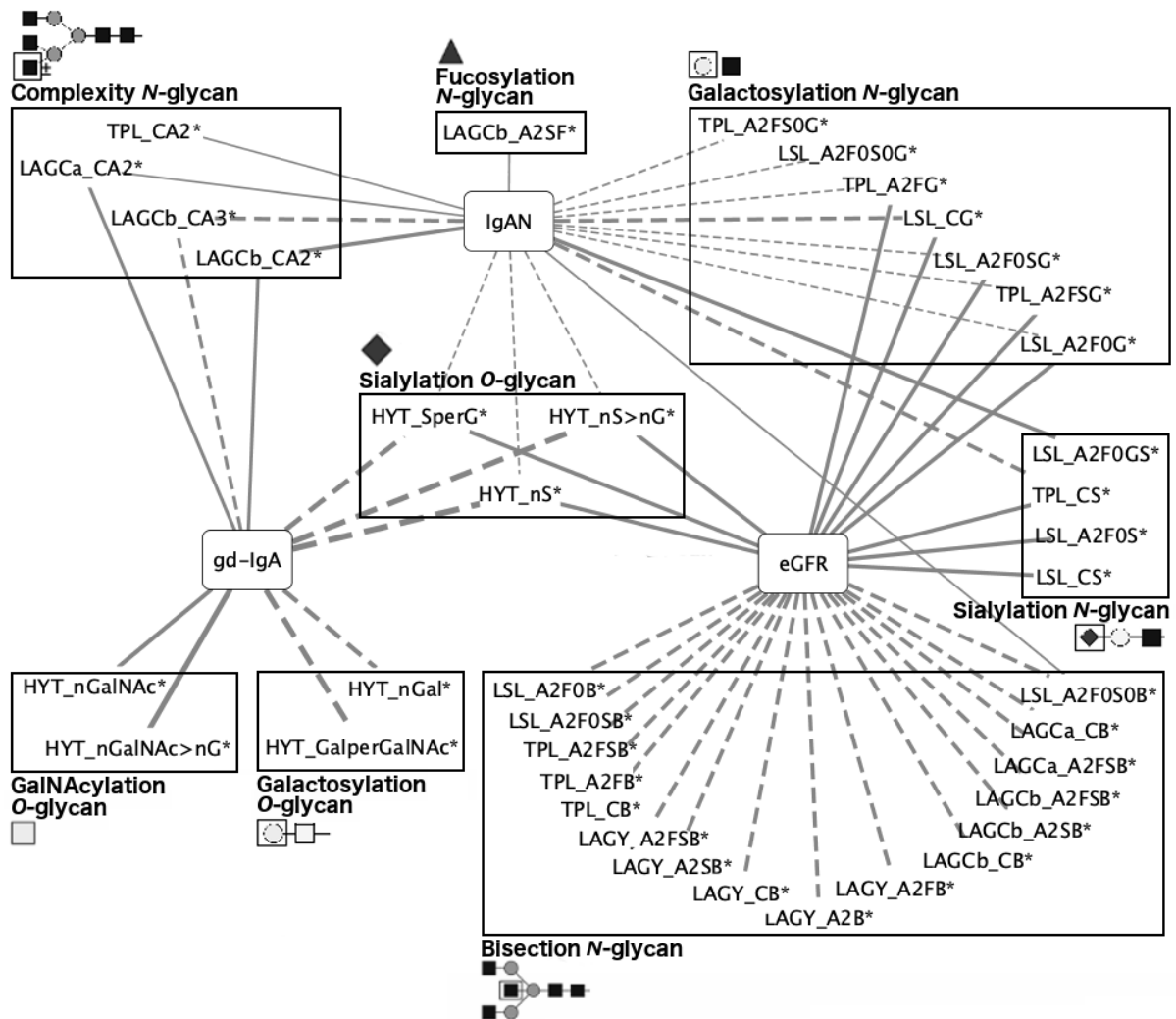


Figure 5. Summary of the associations of derived IgA glycan traits with gd-IgA levels, IgAN, and glomerular function. Line thickness represents effect size (the thicker the line, the stronger the effect's absolute value). Solid lines: positive associations; dotted lines: negative associations. Derived traits are grouped by glycosylation features along with their structural representations. Monosaccharide symbols are depicted, in black and white, according to the nomenclature of the Consortium for Functional Glycomics, and were generated using GlycoWorkbench (56). Complete summary statistics are reported in Supplemental Tables 4, 6, and 7.

Discussion

This study is the first detailed report on site-specific *O*- and *N*-glycosylation signatures of serum IgA1 and IgA2 in IgAN. We analysed a reasonably large cohort of 83 patients and 244 age- and sex-matched controls. Our high-resolution MS-based method features the relative quantitation of, in total, 69 *O*- and *N*-glycopeptide species, further summarized in 52 derived traits. Our data revealed disease associations with *O*-glycan sialylation and with all main *N*-glycosylation features, which include complexity, bisection, galactosylation, fucosylation, and sialylation.

Altered glycosylation of IgA1 *O*-glycans in IgAN is widely reported. Our MS data reflect relative shifts of different glycosylation features due to total area normalization within a glycopeptide cluster. This is different to terminal GalNAc abundance detected by the lectin-based gd-IgA assay. Nevertheless, our MS data on relative *O*-glycan galactosylation, and on the relative abundance of GalNAc on *O*-glycopeptides, can be related to the traditional lectin-based detection of truncated *O*-glycans with terminal GalNAc (GalNAc α 1-Ser/Thr; Tn antigen). Both gd-IgA and IgA titers represent absolute

concentrations but become more comparable to our relative quantitation of MS data when gd-IgA is adjusted for IgA titers. Accordingly, we found a strong positive association of HAA lectin binding with the glycosylation trait *HYT_nGalNAc>nG* which reflects the presence of terminal GalNAc, and, consequently, a negative association with hinge-region galactosylation (*HYT_GalperGalNAc*, *HYT_nGal*) that is supposed to cap the HAA binding motif. Similarly, sialylation (*HYT_nS>nG*) was also inversely associated with gd-IgA level. This can partly be explained by the fact that terminal α 2,3-linked sialic acids can only be present when a galactose has been attached to the core GalNAc. This could also be explained by virtue of the lectin-based assay simply detecting gd-IgA as exposed GalNAc. In 2017, the first GWAS for aberrant *O*-glycosylation of IgA1 identified variants in the *C1GALT1* and *C1GALT1C1* genes that had large effects on gd-IgA1 levels (31). These genes respectively encode the enzyme core 1 β 1–3-galactosyltransferase (C1GalT1) and COSMC, its molecular chaperone – molecular partners that are essential for the galactosylation of IgA1 *O*-glycans (32). Decreased expression and activity of C1GalT1 has been demonstrated in the B Cells of patients with IgAN (33–35). Further studies have also demonstrated that genetic variation at *C1GALT1* influences gd-IgA level (36,37). A recent study has also shown that decreased expression of Golgi matrix protein GM130, which is involved in glycosyltransferase tethering, is associated with reduced C1GalT1 protein level and increased galactose deficiency of IgA1 (38). It is therefore likely that downregulated expression of *C1GALT1* in IgAN patients leads to reduced levels of galactosylation and subsequent reduced levels of sialylation and increased levels of exposed GalNAc, as detected in the lectin-ELISA and reflected in our results.

The relative abundance of sialic acids was the only derived *O*-glycosylation trait that associated with IgAN and renal decline in IgAN patients. Our data suggest that decreased sialylation may also lead to increased presentation of terminal GalNAc, as lower sialylation significantly correlates with higher gd-IgA levels. It is unclear from our study if decreased sialylation is an alteration of IgA glycosylation in itself, or a product of reduced galactosylation. Data on *O*-linked sialylation in IgAN is conflicting. In agreement with our findings two small-scale MS-based studies without quantitation reported decreased numbers of galactose, GalNAc and especially sialic acid residues, in both glomerular and serum IgA1 in pooled samples from IgAN patients as compared to control serum pools (39,40). Conversely, increased expression of *ST6GALNAC2*, a gene encoding an enzyme that mediates sialylation of *O*-glycans, has been reported to be positively correlated with IgAN (41). Interestingly, increased expression of another enzyme, ST6Gal1, correlates with gd-IgA levels (42). Further studies are required to disentangle the relationship between sialylation and IgAN.

Regarding serum IgA *N*-glycosylation in IgAN, only a few small studies exist, and the possible implication of *N*-glycosylation in pathogenesis or renal decline is unknown. Here, we present the first detailed report on associations between serum IgA *N*-glycan galactosylation, sialylation, bisection and fucosylation with IgAN and related clinical parameters. Previously, lower IgA1 Fc-region galactosylation and lower IgA2 sialylation in IgAN patients were detected by lectin-based assays (43). Intriguingly, our findings of decreased *N*-linked sialylation and galactosylation, and increased bisection in IgAN and with worsening renal function, are similar to the *N*-glycosylation differences reported for human salivary vs plasma IgA (25). With this in mind, it is possible that our findings might partly reflect a disease-related increase of IgA molecular species connected to mucosal immune response, which has previously been suggested for IgAN (44).

It is also feasible that our results could reflect a causal relationship of IgA *N*-glycosylation and IgAN pathogenesis via increased formation of polymeric IgA. In comparison to monomeric, polymeric IgA is increased in IgAN patients and it has been implicated in higher immune complex formation and glomerular deposition (45). Strikingly, mice with impaired terminal *N*-glycan galactosylation due to a

knock-out of the β 4-galactosyltransferase I gene were shown to develop human IgAN-like glomerular lesions, with an increased serum IgA, especially the polymeric form (19). Our finding of decreased sialylation in IgAN and with worsening renal function might also reflect a higher abundance of polymeric IgA, which was reported to exhibit a lower degree of sialylation compared to its monomeric form, and thereby enhance binding to mannose-binding lectin as well as to mesangial cells (46–48). Similarly, a higher abundance of fucose and terminal GlcNAc (*e.g.*, bisecting GlcNAc or ungalactosylated antenna GlcNAc) might also be involved in enhanced binding to mannose-binding lectin and subsequent complement activation via the lectin pathway (48). Desialylation and to a lesser extent, additional degalactosylation, has been shown to enhance the binding of polymeric IgA1 to human mesangial cells, as compared to untreated IgA1 *in vitro* (49). Of note, it is unclear to which extent this effect was attributed to *O*- or *N*-glycosylation, or a combination thereof. Notably, the *ST6GAL1* gene, coding for an enzyme responsible for the terminal sialylation of *N*-glycans on different proteins including IgA, was associated with IgAN in Han Chinese (50).

Large-scale *O*-glycomic studies, other than the one reported here and a site-specific *O*- and *N*-glycosylation associations study with rheumatoid arthritis (24), are hitherto lacking due to the technologically challenging nature of these studies. Although a few reports do exist which associate *N*-glycosylation of immunoglobulin G with kidney disease or glomerular function (51–53), none is available for IgAN, hampering our ability to compare IgAN glycosylation signatures displayed by different molecules. Analogously, linking phenotypic associations of the total plasma *N*-glycome with those found here for IgA glycosylation is complicated as many different glycoproteins contribute to the total plasma *N*-glycome, with mostly overlapping structures (54). An analysis of total serum glycans in kidney disease showed eGFR to be associated with higher absolute levels of biantennary digalactosylated disialylated glycans with and without bisection (53) yet information on the glycoproteins and glycosylation sites contributing to this signature is lacking. In comparison, our novel approach for specific IgA glycosylation analysis presented here provides these extra layers of information by covering all main glycosylation features present on 69 measured glycopeptides of IgA (54).

We have made a first attempt to elucidate the complex *O*- and *N*-glycosylation of human serum IgA in relation to IgAN in a comprehensive fashion with direct detection employing high-resolution mass spectrometry. Due to the small sample size, we could not build and validate a predictive model for IgAN pathogenesis and renal decline. However, we have shown that directly measured glycopeptide level IgA glycosylations are better predictors of both IgAN status and renal function than gd-IgA levels alone. Our results widen the current view on the potential role of IgA glycosylation in IgAN pathogenesis and in renal decline and open new opportunities for investigations on glycopeptides as potential biomarkers for disease onset and progression. We envisage that these results, together with the increasing interest in the use of glycomics in clinical settings, will encourage increased inclusion of IgA glycomics in studies, which will promote the development of targeted analysis panels and of absolute quantification approaches, currently hindered by the lack of stable isotope-labeled glycopeptide standards.

In summary, we provide the first evidence of a possible role for IgA *N*-glycosylation in IgAN pathogenesis, which should be taken forward in mechanistic studies and could result in novel therapeutic and preventive approaches in the future.

Author contributions

MW and MF designed the study. HJLB, NRMT, HTC, and MCP collected the samples and clinical data in the Causes and Predictors of Outcome in IgA Nephropathy Study. HJLB measured serum IgA and gd-IgA levels. ALHE optimized the LC-MS method. FC and ALHE performed IgA glycopeptide analysis by mass spectrometry. FC processed the raw data and calculated the derived traits. AV carried out the statistical analyses. VD, AV, HJLB, FC, MW, and MF interpreted the results. FC generated the figures for the glycopeptides and derived traits. AV generated the figures for the association study results. AV and MF generated the figures summarising the association results. VD, AV, HJLB, FC, and MF drafted the manuscript. All authors approved the final version of the manuscript.

Acknowledgments

TwinsUK is funded by the Wellcome Trust, Medical Research Council, European Union, Chronic Disease Research Foundation (CDRF), the National Institute for Health Research (NIHR)-funded BioResource, Clinical Research Facility and Biomedical Research Centre based at Guy's and St Thomas' NHS Foundation Trust in partnership with King's College London. We acknowledge support by the National Institute for Health Research Biomedical Research Centre based at Imperial College Healthcare National Health Service Trust and Imperial College London, and from the National Institute for Health Research Clinical Research Network. The views expressed are those of the authors and not necessarily those of the National Health Service, the National Institute for Health Research, or the Department of Health.

Funding

This work was supported by funding from the Medical Research Council (MR/K01353X/1). MCP is a Wellcome Trust Senior Fellow in Clinical Science (212252/Z/18/Z).

Disclosures

The authors have nothing to disclose.

Data Sharing Statement

Data on study participants are available to *bona fide* researchers under managed access due to governance and ethical constraints. IgAN patients' raw data should be requested via contact with the corresponding author. Twins' raw data should be requested via the TwinsUK website (<http://twinsuk.ac.uk/resources-for-researchers/access-our-data/>), and requests are reviewed by the TwinsUK Resource Executive Committee (TREC) regularly.

Supplemental material Table of Content:

Supplemental Methods. IgA glycopeptide analysis by mass spectrometry.

Supplemental Figure 1. Age distribution and sex proportion for the study sample.

Supplemental Figure 2. Selected associations between derived *O*-glycosylation traits, and gd-IgA1 levels detected by HAA lectin in 83 IgAN patients. Quantile-normalised age- and sex-corrected values are plotted, values are plotted, and each scatterplot reports effect size (β), standard error (SE), and p-value (P) of the linear regression analysis. Derived traits HYT_nS, HYT_nGal, and HYT_nGalNAc correspond to average number of sialic acids, galactoses, and *N*-acetylgalactosamines, respectively. Monosaccharide symbols are depicted, in black and white, according with the nomenclature of the Consortium for Functional Glycomics, and were generated using GlycoWorkbench [doi: 10.1021/pr7008252].

Supplemental Figure 3. Summary of the associations of measured IgA glycopeptides with gd-IgA levels, IgAN, and glomerular function. Left Panel: *O*-glycans; right panel: *N*-glycans. Line thickness represents effect size (the thicker the line, the stronger the effect absolute value). Solid lines represent positive associations, dotted lines represent negative associations. Complete summary statistics are reported in Supplemental Tables 4, 6, and 7.

Supplemental Table 1. Phenotypic details of the study sample. Differences in age and gd-IgA distribution, and in sex proportions were evaluated using Wilcoxon's rank sum test and Pearson's χ^2 test, respectively.

Supplemental Table 2. Analytical characteristics of the detected glycopeptides per glycosylation site. The proposed structures are based on previously reported literature as referenced in the manuscript Methods section. Repeatability of relative intensity and of the average number of monosaccharides are reported for 22 plasma standard replicates.

Supplemental Table 3. Derived IgA glycosylation traits calculated from detected glycopeptides (see Supplemental Table 2) with their technical (n = 22) vs biological variation (83 IgAN cases and 244 healthy controls).

Supplemental Table 4. Associations of IgA glycosylation with gd-IgA in healthy controls. Significant associations passing a Bonferroni-derived p-value of 7.3×10^{-4} and 1.0×10^{-3} for measured and derived traits, respectively, are presented using a bold font-face. Associations were corrected for age, sex, their interaction term, and for family structure. The table reports the number of individuals in the dataset (N), the effect size (Beta) along with its standard error (SE) and association p-value (P). *indicates a derived trait.

Supplemental Table 5. Associations of IgA glycosylation with gd-IgA with IgA1 titer correction in a subset of healthy controls. Significant associations passing a Bonferroni-derived p-value of 2.2×10^{-3} and 3.1×10^{-3} for measured and derived traits, respectively, are represented using a bold font-face. Associations were corrected for age, sex, their interaction term, and for family structure. The table reports number of individuals in the dataset (N), the effect size (Beta) along with its standard error (SE) and association p-value (P). * indicates a derived trait.

Supplemental Table 6. Case-control association study of IgA glycosylation. Significant associations passing a Bonferroni-derived p-value of 7.3×10^{-4} and 1.0×10^{-3} for measured and derived traits, respectively, are presented using a bold font-face. Associations were corrected for age, sex, their interaction term, and for family structure. The table reports the number of individuals in the dataset (N), the effect size (Beta) along with its standard error (SE) and association p-value (P). *indicates a derived trait.

Supplemental Table 7. Associations of IgA glycosylation with eGFR in IgAN patients. Significant associations passing a Bonferroni-derived p-value of 7.3×10^{-4} and 1.0×10^{-3} for measured and derived traits, respectively, are presented using a bold font-face. Associations were corrected for age, sex, and their interaction term. The table reports the number of individuals in the dataset (N), the effect size (Beta) along with its standard error (SE) and association p-value (P). *indicates a derived trait.

References

1. Schena FP, Nistor I: Epidemiology of IgA Nephropathy: A Global Perspective. *Semin Nephrol* 38: 435–442, 2018
2. Berthoux FC, Mohey H, Afiani A: Natural History of Primary IgA Nephropathy. *Semin Nephrol* 28: 4–9, 2008
3. Jennette JC: The Immunohistology of IgA Nephropathy. *Am J Kidney Dis* 12: 348–352, 1988
4. Suzuki H, Kiryluk K, Novak J, Moldoveanu Z, Herr AB, Renfrow MB, Wyatt RJ, Scolari F, Mestecky J, Gharavi AG, Julian BA: The Pathophysiology of IgA Nephropathy. *J Am Soc Nephrol* 22: 1795–1803, 2011
5. Kerr MA: The structure and function of human IgA. *Biochem J* 271: 285–296, 1990
6. Mattu TS, Pleass RJ, Willis AC, Kilian M, Wormald MR, Lellouch AC, Rudd PM, Woof JM, Dwek RA: The Glycosylation and Structure of Human Serum IgA1, Fab, and Fc Regions and the Role of N-Glycosylation on Fc α Receptor Interactions. *J Biol Chem* 273: 2260–2272, 1998
7. Tarelli E, Smith AC, Hendry BM, Challacombe SJ, Pouria S: Human serum IgA1 is substituted with up to six O-glycans as shown by matrix assisted laser desorption ionisation time-of-flight mass spectrometry. *Carbohydr Res* 339: 2329–2335, 2004
8. Woof JM, Russell MW: Structure and function relationships in IgA. *Mucosal Immunol* 4: 590–597, 2011
9. Mestecky J, Tomana M, Crowley-Nowick PA, Moldoveanu Z, Julian BA, Jackson S: Defective Galactosylation and Clearance of IgA1 Molecules as a Possible Etiopathogenic Factor in IgA Nephropathy1 [Internet]. In: *Contributions to Nephrology*, edited by B□n□ MC, Faure G, Kessler M, pp 172–182, 1993 Available from: <https://www.karger.com/Article/FullText/422410> [cited 2021 Feb 19]
10. Moldoveanu Z, Wyatt RJ, Lee JY, Tomana M, Julian BA, Mestecky J, Huang W-Q, Anreddy SR, Hall S, Hastings MC, Lau KK, Cook WJ, Novak J: Patients with IgA nephropathy have increased serum galactose-deficient IgA1 levels. *Kidney Int* 71: 1148–1154, 2007
11. Sun Q, Zhang Z, Zhang H, Liu X: Aberrant IgA1 Glycosylation in IgA Nephropathy: A Systematic Review. *PLOS ONE* 11: e0166700, 2016
12. Medjeral-Thomas NR, Lomax-Browne HJ, Beckwith H, Willicombe M, McLean AG, Brookes P, Pusey CD, Falchi M, Cook HT, Pickering MC: Circulating complement factor H-related proteins 1 and 5 correlate with disease activity in IgA nephropathy. *Kidney Int* 92: 942–952, 2017
13. Hastings MC, Moldoveanu Z, Julian BA, Novak J, Sanders JT, McGlothlan KR, Gharavi AG, Wyatt RJ: Galactose-Deficient IgA1 in African Americans with IgA Nephropathy: Serum Levels and Heritability. *Clin J Am Soc Nephrol* 5: 2069–2074, 2010
14. Tachibana K, Nakamura S, Wang H, Iwasaki H, Tachibana K, Maebara K, Cheng L, Hirabayashi J, Narimatsu H: Elucidation of binding specificity of Jacalin toward O-glycosylated peptides: quantitative analysis by frontal affinity chromatography. *Glycobiology* 16: 46–53, 2006
15. Moore JS, Kulhavy R, Tomana M, Moldoveanu Z, Suzuki H, Brown R, Hall S, Kilian M, Poulsen K, Mestecky J, Julian BA, Novak J: Reactivities of N-acetylgalactosamine-specific lectins with human IgA1 proteins. *Mol Immunol* 44: 2598–2604, 2007
16. Yasutake J, Suzuki Y, Suzuki H, Hiura N, Yanagawa H, Makita Y, Kaneko E, Tomino Y: Novel lectin-independent approach to detect galactose-deficient IgA1 in IgA nephropathy. *Nephrol Dial Transplant* 30: 1315–1321, 2015
17. Linossier M-T, Palle S, Berthoux F: Different glycosylation profile of serum IgA1 in IgA nephropathy according to the glomerular basement membrane thickness: Normal versus thin. *Am J Kidney Dis* 41: 558–564, 2003

18. Amore A, Cirina P, Conti G, Brusa P, Peruzzi L, Coppo R: Glycosylation of circulating IgA in patients with IgA nephropathy modulates proliferation and apoptosis of mesangial cells. *J Am Soc Nephrol JASN* 12: 1862–1871, 2001
19. Nishie T, Miyaishi O, Azuma H, Kameyama A, Naruse C, Hashimoto N, Yokoyama H, Narimatsu H, Wada T, Asano M: Development of Immunoglobulin A Nephropathy- Like Disease in β -1,4-Galactosyltransferase-I-Deficient Mice. *Am J Pathol* 170: 447–456, 2007
20. Andrew T, Hart DJ, Snieder H, de Lange M, Spector TD, MacGregor AJ: Are twins and singletons comparable? A study of disease-related and lifestyle characteristics in adult women. *Twin Res* 4: 464–477, 2001
21. Lomax-Browne HJ, Visconti A, Pusey CD, Cook HT, Spector TD, Pickering MC, Falchi M: IgA1 Glycosylation Is Heritable in Healthy Twins. *J Am Soc Nephrol* 28: 64–68, 2017
22. Falck D, Jansen BC, de Haan N, Wuhrer M: High-Throughput Analysis of IgG Fc Glycopeptides by LC-MS. *Methods Mol Biol Clifton NJ* 1503: 31–47, 2017
23. Jansen BC, Falck D, de Haan N, Hipgrave Ederveen AL, Razdorov G, Lauc G, Wuhrer M: LaCyTools: A Targeted Liquid Chromatography–Mass Spectrometry Data Processing Package for Relative Quantitation of Glycopeptides. *J Proteome Res* 15: 2198–2210, 2016
24. Bondt A, Nicolardi S, Jansen BC, Kuijper TM, Hazes JMW, van der Burgt YEM, Wuhrer M, Dolhain RJEM: IgA N- and O-glycosylation profiling reveals no association with the pregnancy-related improvement in rheumatoid arthritis. *Arthritis Res Ther* 19: 160, 2017
25. Plomp R, de Haan N, Bondt A, Murli J, Dotz V, Wuhrer M: Comparative Glycomics of Immunoglobulin A and G From Saliva and Plasma Reveals Biomarker Potential. *Front Immunol* 9: 2436, 2018
26. Bondt A, Nicolardi S, Jansen BC, Stavenhagen K, Blank D, Kammeijer GSM, Kozak RP, Fernandes DL, Hensbergen PJ, Hazes JMW, van der Burgt YEM, Dolhain RJEM, Wuhrer M: Longitudinal monitoring of immunoglobulin A glycosylation during pregnancy by simultaneous MALDI-FTICR-MS analysis of N- and O-glycopeptides. *Sci Rep* 6: 27955, 2016
27. Gudelj I, Lauc G, Pezer M: Immunoglobulin G glycosylation in aging and diseases. *Cell Immunol* 333: 65–79, 2018
28. Cohen J: Statistical power analysis for the behavioral sciences. Academic press
29. Li J, Ji L: Adjusting multiple testing in multilocus analyses using the eigenvalues of a correlation matrix. *Heredity* 95: 221–227, 2005
30. McFadden D: Conditional logit analysis of qualitative choice behavior. *Front Econom* 105–142, 1974
31. Kiryluk K, Li Y, Moldoveanu Z, Suzuki H, Reily C, Hou P, Xie J, Mladkova N, Prakash S, Fischman C, Shapiro S, LeDesma RA, Bradbury D, Ionita-Laza I, Eitner F, Rauen T, Maillard N, Berthoux F, Floege J, Chen N, Zhang H, Scolari F, Wyatt RJ, Julian BA, Gharavi AG, Novak J: GWAS for serum galactose-deficient IgA1 implicates critical genes of the O-glycosylation pathway. *PLOS Genet* 13: e1006609, 2017
32. Ju T, Cummings RD: A unique molecular chaperone Cosmc required for activity of the mammalian core 1 3-galactosyltransferase. *Proc Natl Acad Sci* 99: 16613–16618, 2002
33. Allen AC, Topham PS, Harper SJ, Feehally J: Leucocyte beta 1,3 galactosyltransferase activity in IgA nephropathy. *Nephrol Dial Transplant* 12: 701–706, 1997
34. Suzuki H, Moldoveanu Z, Hall S, Brown R, Vu HL, Novak L, Julian BA, Tomana M, Wyatt RJ, Edberg JC, Alarcón GS, Kimberly RP, Tomino Y, Mestecky J, Novak J: IgA1-secreting cell lines from patients with IgA nephropathy produce aberrantly glycosylated IgA1. *J Clin Invest* JCI33189, 2008

35. Xing Y, Li L, Zhang Y, Wang F, He D, Liu Y, Jia J, Yan T, Lin S: C1GALT1 expression is associated with galactosylation of IgA1 in peripheral B lymphocyte in immunoglobulin a nephropathy. *BMC Nephrol* 21: 18, 2020
36. Gale DP, Molyneux K, Wimbury D, Higgins P, Levine AP, Caplin B, Ferlin A, Yin P, Nelson CP, Stanescu H, Samani NJ, Kleta R, Yu X, Barratt J: Galactosylation of IgA1 Is Associated with Common Variation in *C1GALT1*. *J Am Soc Nephrol* 28: 2158–2166, 2017
37. Wang Y-N, Zhou X-J, Chen P, Yu G-Z, Zhang X, Hou P, Liu L-J, Shi S-F, Lv J-C, Zhang H: Interaction between *GALNT12* and *C1GALT1* Associates with Galactose-Deficient IgA1 and IgA Nephropathy. *J Am Soc Nephrol* ASN.2020060823, 2021
38. Wang C, Ye M, Zhao Q, Xia M, Liu D, He L, Chen G, Peng Y, Liu H: Loss of the Golgi Matrix Protein 130 Cause Aberrant IgA1 Glycosylation in IgA Nephropathy. *Am J Nephrol* 49: 307–316, 2019
39. Hiki Y, Odani H, Takahashi M, Yasuda Y, Nishimoto A, Iwase H, Shinzato T, Kobayashi Y, Maeda K: Mass spectrometry proves under-O-glycosylation of glomerular IgA1 in IgA nephropathy. *Kidney Int* 59: 1077–1085, 2001
40. Odani H, Hiki Y, Takahashi M, Nishimoto A, Yasuda Y, Iwase H, Shinzato T, Maeda K: Direct Evidence for Decreased Sialylation and Galactosylation of Human Serum IgA1 Fc O-Glycosylated Hinge Peptides in IgA Nephropathy by Mass Spectrometry. *Biochem Biophys Res Commun* 271: 268–274, 2000
41. Suzuki H, Moldoveanu Z, Julian BA, Wyatt RJ, Novak J: Autoantibodies Specific for Galactose-Deficient IgA1 in IgA Vasculitis With Nephritis. *Kidney Int Rep* 4: 1717–1724, 2019
42. Liu Y, Wang F, Zhang Y, Jia J, Yan T: ST6Gal1 is up-regulated and associated with aberrant IgA1 glycosylation in IgA nephropathy: An integrated analysis of the transcriptome. *J Cell Mol Med* 24: 10493–10500, 2020
43. Baharaki D, Dueymes M, Perrichot R, Basset C, le Corre R, Cledes J, Youinou P: Aberrant glycosylation of IgA from patients with IgA nephropathy. *Glycoconj J* 13: 505–511, 1996
44. Knoppova B, Reily C, Maillard N, Rizk DV, Moldoveanu Z, Mestecky J, Raska M, Renfrow MB, Julian BA, Novak J: The Origin and Activities of IgA1-Containing Immune Complexes in IgA Nephropathy. *Front Immunol* 7: 117, 2016
45. Leung JCK, Tang SCW, Lam MF, Chan TM, Lai KN: Charge-dependent binding of polymeric IgA1 to human mesangial cells in IgA nephropathy. *Kidney Int* 59: 277–285, 2001
46. Lombana TN, Rajan S, Zorn JA, Mandikian D, Chen EC, Estevez A, Yip V, Bravo DD, Phung W, Farahi F, Viajar S, Lee S, Gill A, Sandoval W, Wang J, Ciferri C, Boswell CA, Matsumoto ML, Spiess C: Production, characterization, and *in vivo* half-life extension of polymeric IgA molecules in mice. *mAbs* 11: 1122–1138, 2019
47. Oortwijn BD, Roos A, Royle L, van Gijlswijk-Janssen DJ, Faber-Krol MC, Eijgenraam J-W, Dwek RA, Daha MR, Rudd PM, van Kooten C: Differential Glycosylation of Polymeric and Monomeric IgA: A Possible Role in Glomerular Inflammation in IgA Nephropathy. *J Am Soc Nephrol* 17: 3529–3539, 2006
48. Roos A, Bouwman LH, van Gijlswijk-Janssen DJ, Faber-Krol MC, Stahl GL, Daha MR: Human IgA Activates the Complement System Via the Mannan-Binding Lectin Pathway. *J Immunol* 167: 2861–2868, 2001
49. Gao Y-H, Xu L-X, Zhang J-J, Zhang Y, Zhao M-H, Wang H-Y: Differential binding characteristics of native monomeric and polymeric immunoglobulin A1 (IgA1) on human mesangial cells and the influence of *in vitro* deglycosylation of IgA1 molecules: Glycosylation and size of IgA1 affect binding characteristics on HMC. *Clin Exp Immunol* 148: 507–514, 2007

50. Li M, Foo J-N, Wang J-Q, Low H-Q, Tang X-Q, Toh K-Y, Yin P-R, Khor C-C, Goh Y-F, Irwan ID, Xu R-C, Andiappan AK, Bei J-X, Rotzschke O, Chen M-H, Cheng C-Y, Sun L-D, Jiang G-R, Wong T-Y, Lin H-L, Aung T, Liao Y-H, Saw S-M, Ye K, Ebstein RP, Chen Q-K, Shi W, Chew S-H, Chen J, Zhang F-R, Li S-P, Xu G, Shyong Tai E, Wang L, Chen N, Zhang X-J, Zeng Y-X, Zhang H, Liu Z-H, Yu X-Q, Liu J-J: Identification of new susceptibility loci for IgA nephropathy in Han Chinese. *Nat Commun* [Internet] 6: 2015 Available from: <http://www.nature.com/articles/ncomms8270> [cited 2020 Nov 25]
51. Barrios C, Zierer J, Gudelj I, Štambuk J, Ugrina I, Rodríguez E, Soler MJ, Pavić T, Šimurina M, Keser T, Pučić-Baković M, Mangino M, Pascual J, Spector TD, Lauc G, Menni C: Glycosylation Profile of IgG in Moderate Kidney Dysfunction. *J Am Soc Nephrol* 27: 933–941, 2016
52. Bermingham ML, Colombo M, McGurnaghan SJ, Blackbourn LAK, Vučković F, Pučić Baković M, Trbojević-Akmačić I, Lauc G, Agakov F, Agakova AS, Hayward C, Klarić L, Palmer CNA, Petrie JR, Chalmers J, Collier A, Green F, Lindsay RS, Macrury S, McKnight JA, Patrick AW, Thekkepat S, Gornik O, McKeigue PM, Colhoun HM: N-Glycan Profile and Kidney Disease in Type 1 Diabetes. *Diabetes Care* 41: 79–87, 2018
53. Colombo M, Asadi Shehni A, Thoma I, McGurnaghan SJ, Blackbourn LAK, Wilkinson H, Collier A, Patrick AW, Petrie JR, McKeigue PM, Saldova R, Colhoun HM, the Scottish Diabetes Research Network (SDRN) Type 1 Bioresource Investigators: Quantitative levels of serum N-glycans in type 1 diabetes and their association with kidney disease. *Glycobiology* cwa106, 2020
54. Clerc F, Reiding KR, Jansen BC, Kammeijer GSM, Bondt A, Wuhrer M: Human plasma protein N-glycosylation. *Glycoconj J* 33: 309–343, 2016
55. de Haan N, Falck D, Wuhrer M: Monitoring of immunoglobulin N- and O-glycosylation in health and disease. *Glycobiology* 30: 226–240, 2020
56. Ceroni A, Maass K, Geyer H, Geyer R, Dell A, Haslam SM: GlycoWorkbench: A Tool for the Computer-Assisted Annotation of Mass Spectra of Glycans[†]. *J Proteome Res* 7: 1650–1659, 2008